Electronic Supplementary Material (ESI) for Physical Chemistry Chemical Physics

Electronic Supplementary Information for: Incidence angle dependence of enhancement factor in attenuated total reflection surface enhanced infrared absorption spectroscopy studied by numerical solution of the vectorial Maxwell equations

Ganesh Vasan, Andreas Erbe

1 Field images

This section contains electric field patterns which are not included in the main article to keep the manuscript appropriately sized.

Fig. 1 shows the electric field for geometry A under the same conditions as for geometry B as shown in Fig. 6(a) of the main manuscript.

The same results as shown in Fig. 6 of the main article with the same colour scale for all angles of incidence is displayed in Fig. 2.

A comparison of electric field patterns in different planes are shown in Fig. 3-6. Each field image has an individual colour scale. Some images are identical with images shown in the main article, where only cuts in the the decisive planes are shown. Each image shows the total electric field amplitude, i.e. $\sqrt{|E_x|^2 + |E_y|^2 + |E_z|^2}$.

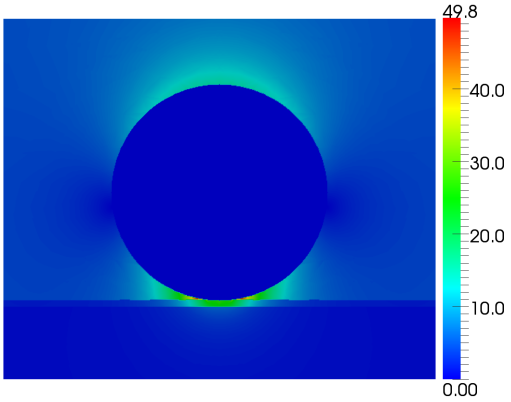

Figure 1: Electric field strength in x-y-plane (incident p-polarisation) at 3200 cm^{-1} in geometry A (diameter 30 nm) at $\theta = 18°$.

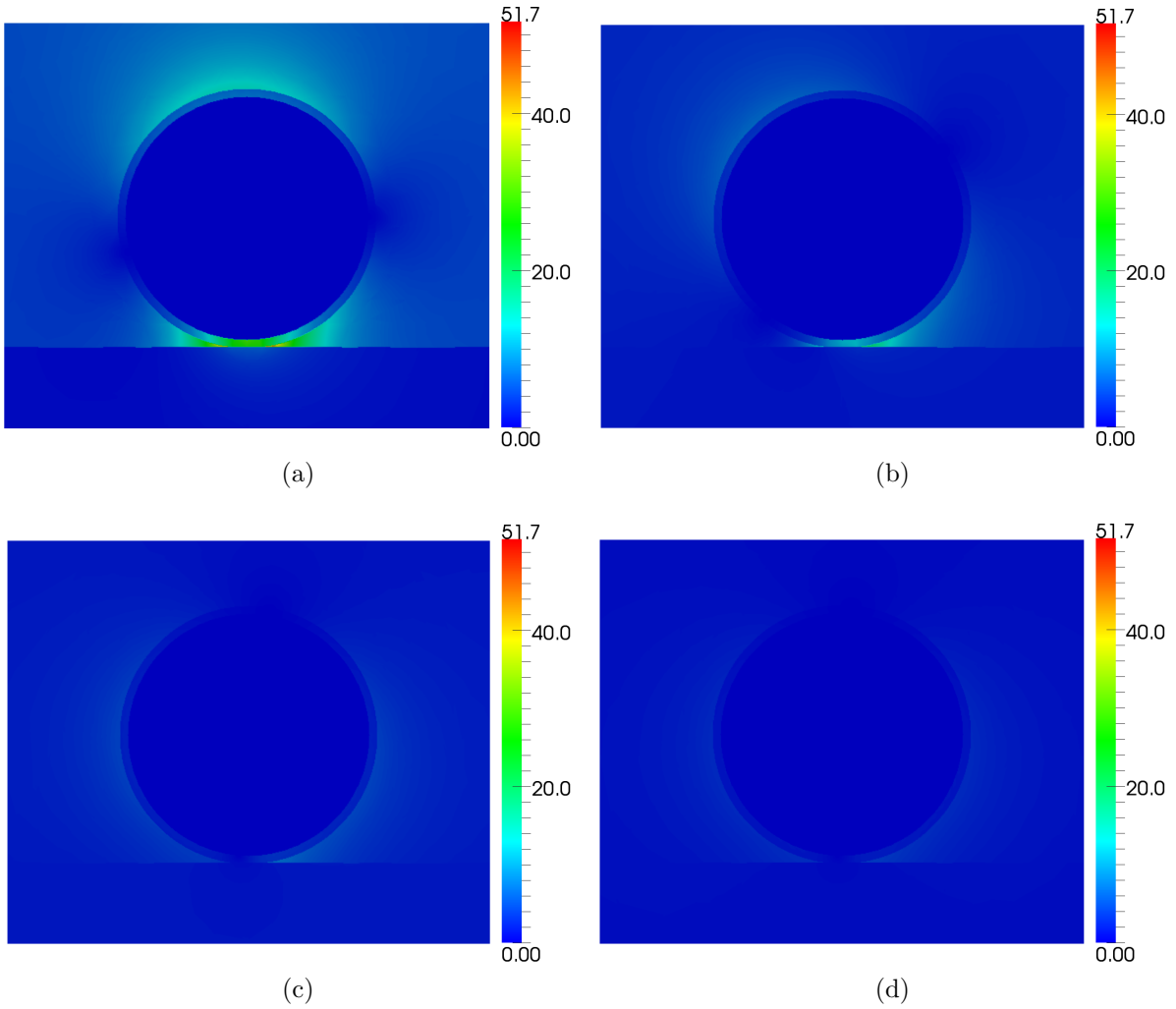

Figure 2: Total electric field amplitude in x-y-plane (incident p-polarisation) at 3200 cm^{-1} around a single coated gold particle (geometry B) of diameter 30 nm with varying θ: 18° (a), 20° (b), 40° (c) and 60° (d). The images show the same results as Fig. 6 in the main article, but here all with the colour scale of the 18° case.

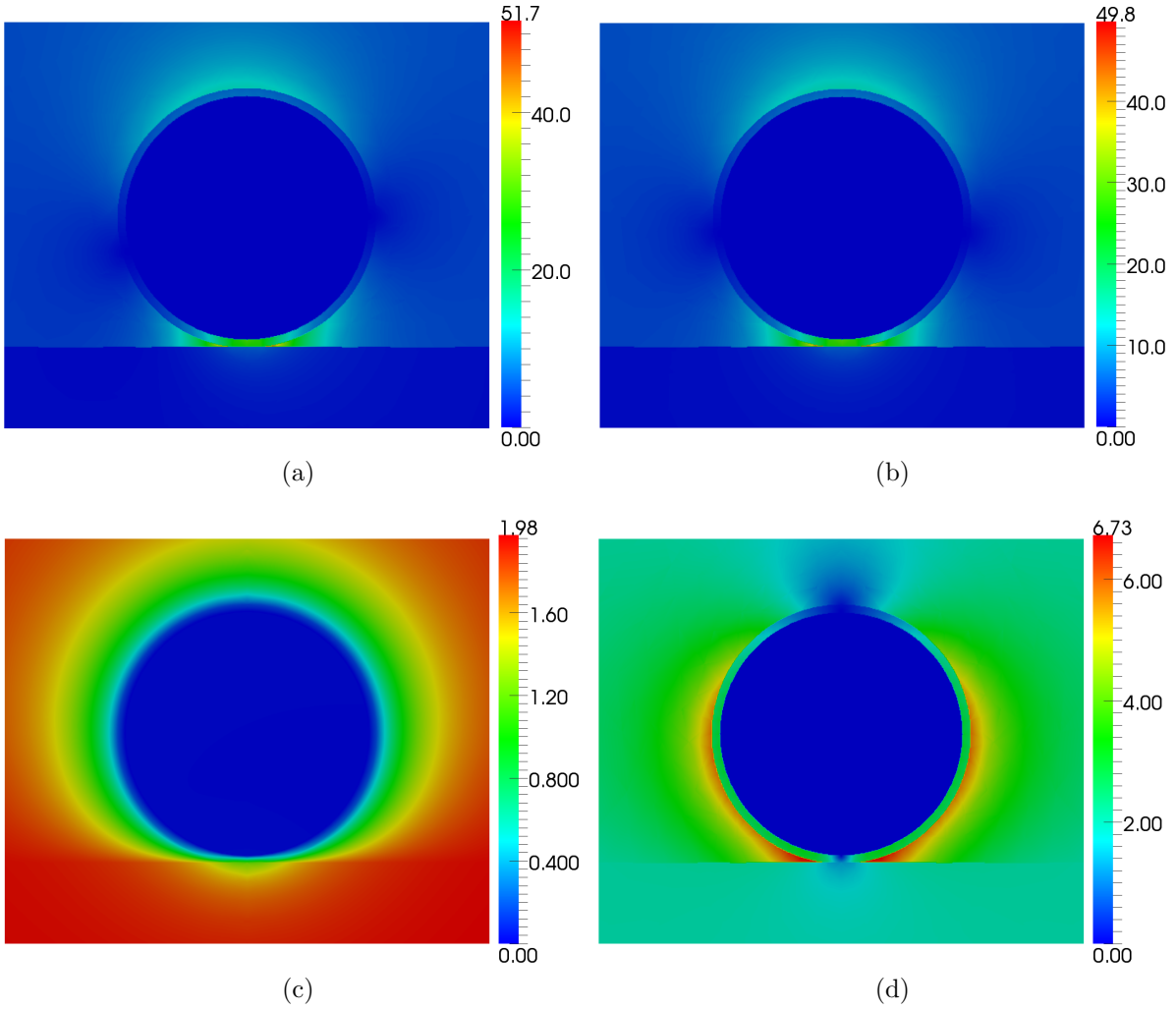

Figure 3: Total electric field amplitude around a single coated gold particle (geometry B) of diameter 30 nm at 3200 cm^{-1} for $\theta = 18°$ in x-y-plane (incident p-polarisation) (a), in y-z-plane (incident p-polarisation) (b), in x-y-plane (incident s-polarisation) (c) and in y-z-plane (incident s-polarisation) (d).

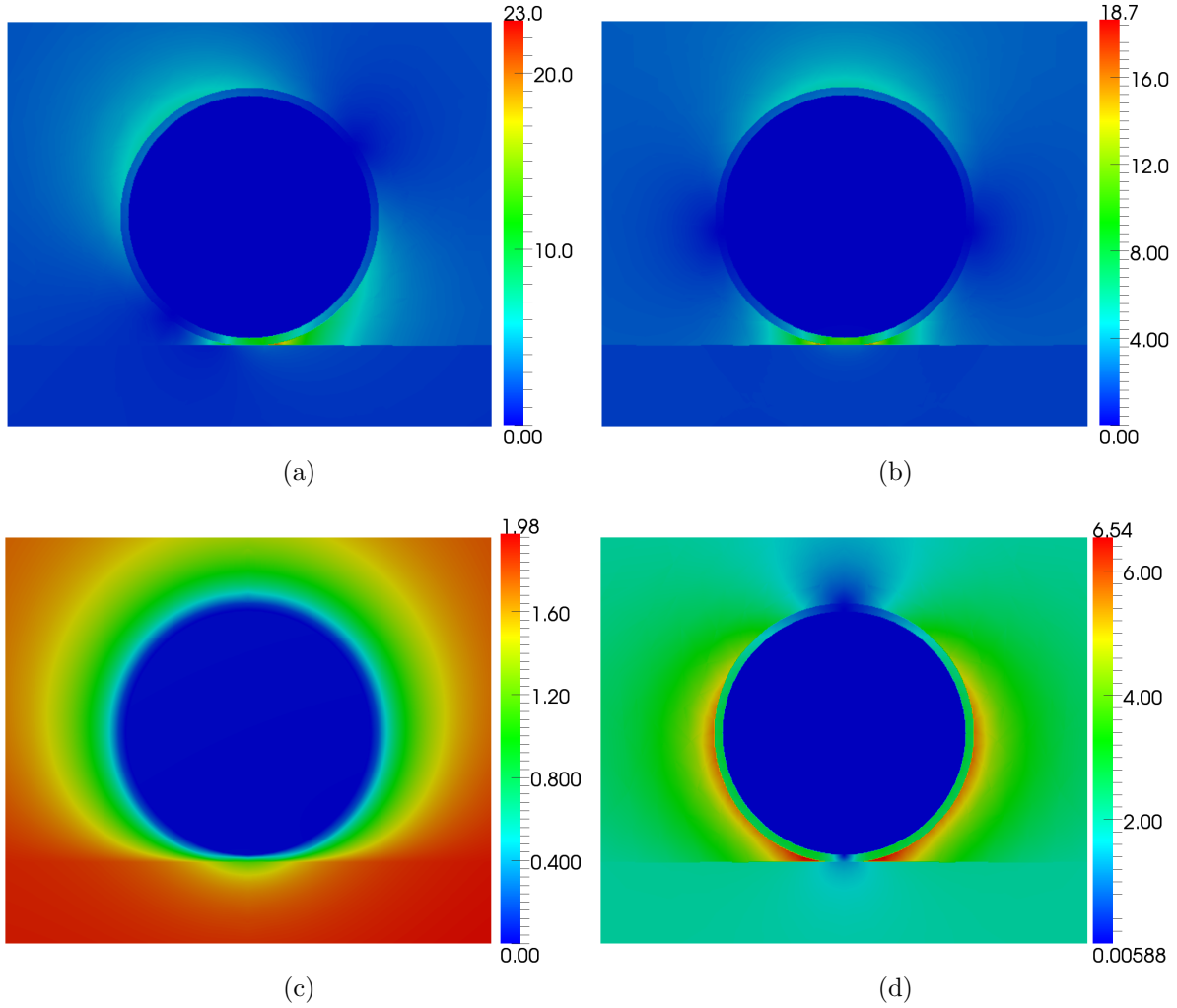

Figure 4: Total electric field amplitude around a single coated gold particle (geometry B) of diameter 30 nm at 3200 cm^{-1} for $\theta = 20°$ in x-y-plane (incident p-polarisation) (a), in y-z-plane (incident p-polarisation) (b), in x-y-plane (incident s-polarisation) (c) and in y-z-plane (incident s-polarisation) (d).

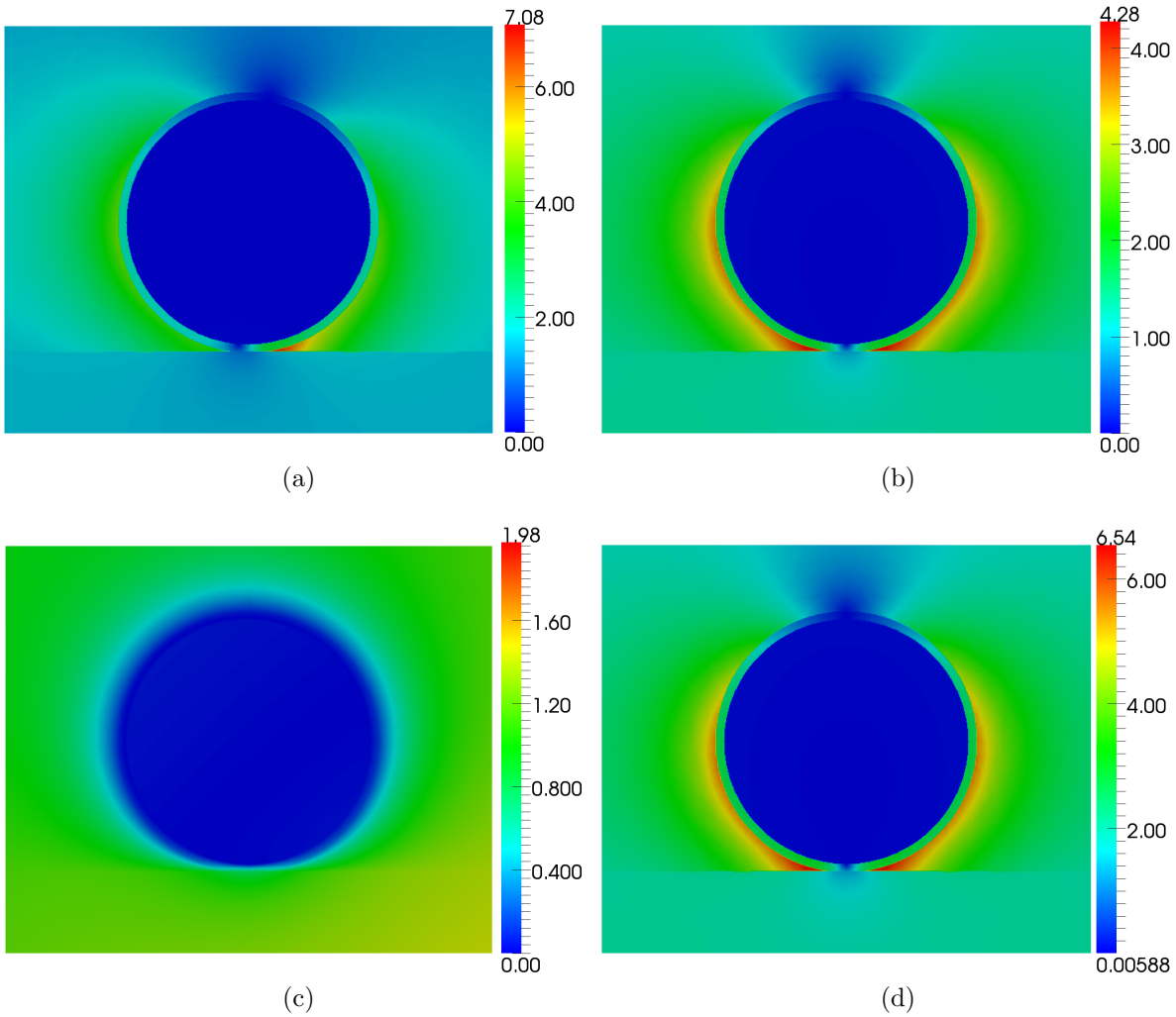

Figure 5: Total electric field amplitude around a single coated gold particle (geometry B) of diameter 30 nm at 3200 cm^{-1} for $\theta = 40°$ in x-y-plane (incident p-polarisation) (a), in y-z-plane (incident p-polarisation) (b), in x-y-plane (incident s-polarisation) (c) and in y-z-plane (incident s-polarisation) (d).

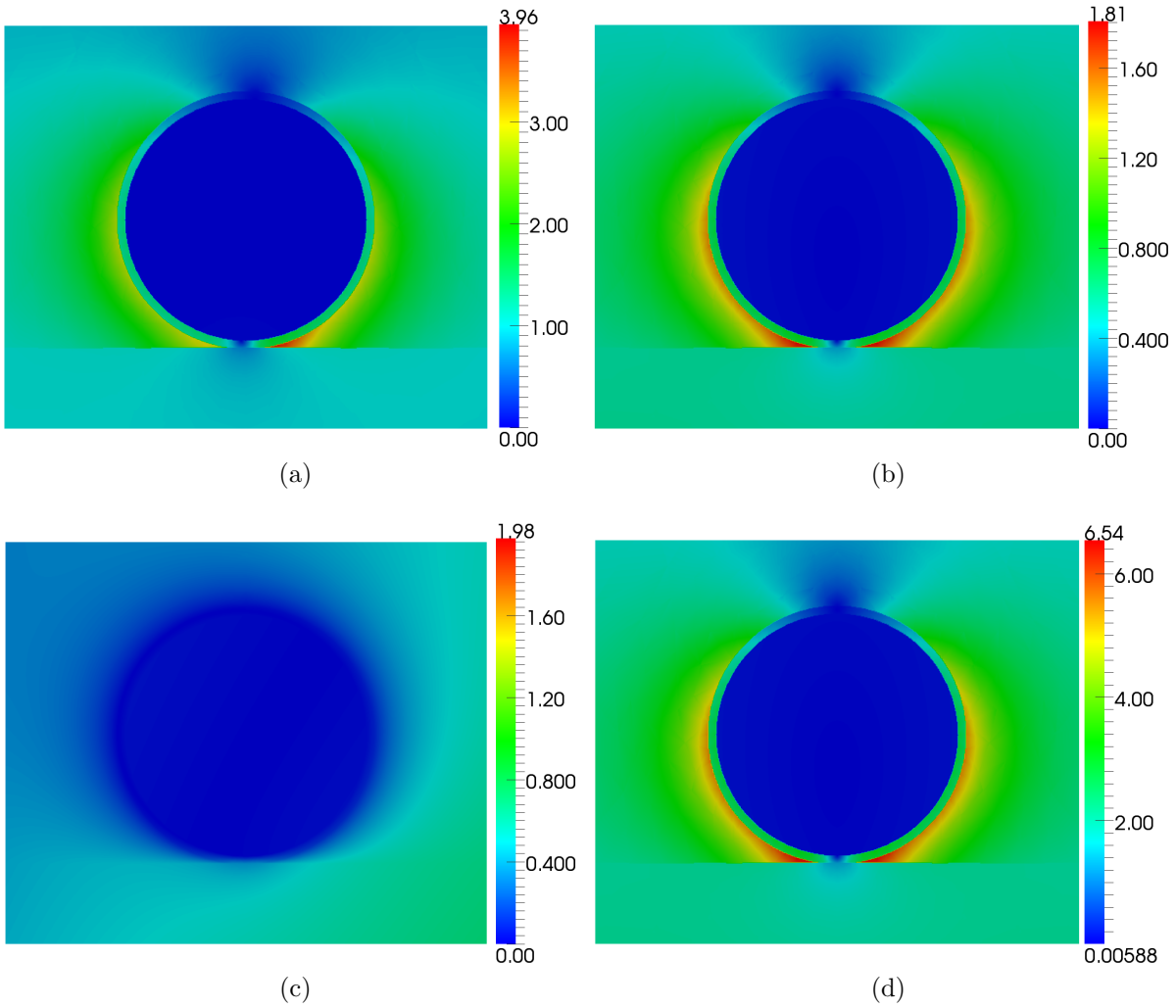

Figure 6: Total electric field amplitude around a single coated gold particle (geometry B) of diameter 30 nm at 3200 cm^{-1} for $\theta = 60°$ in x-y-plane (incident p-polarisation) (a), in y-z-plane (incident p-polarisation) (b), in x-y-plane (incident s-polarisation) (c) and in y-z-plane (incident s-polarisation) (d).

2 Scanning electron micrographs

The particles used for experimental studies in this work have been deposited on an Si-wafer, and inspected using a field emission scanning electron microscope (SEM) ZEISS LEO 1550VP GEMINI. A distribution of diameters is shown in Fig. 7. Micrographs with different magnifications are shown in Fig. 8-11.

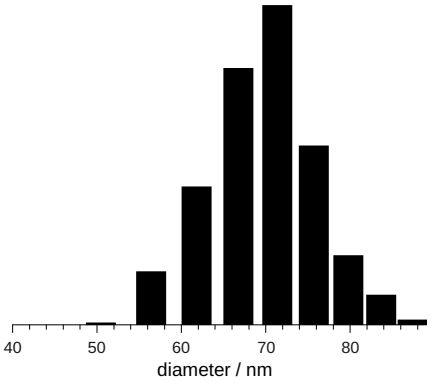

Figure 7: Histogram of diameters.

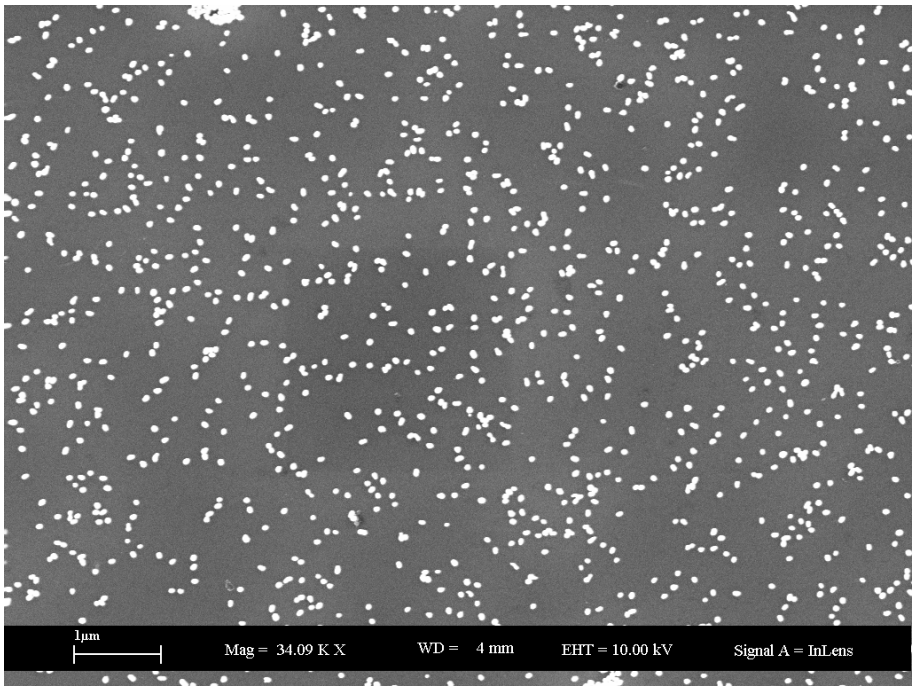

Figure 8: SEM image of the particles used.

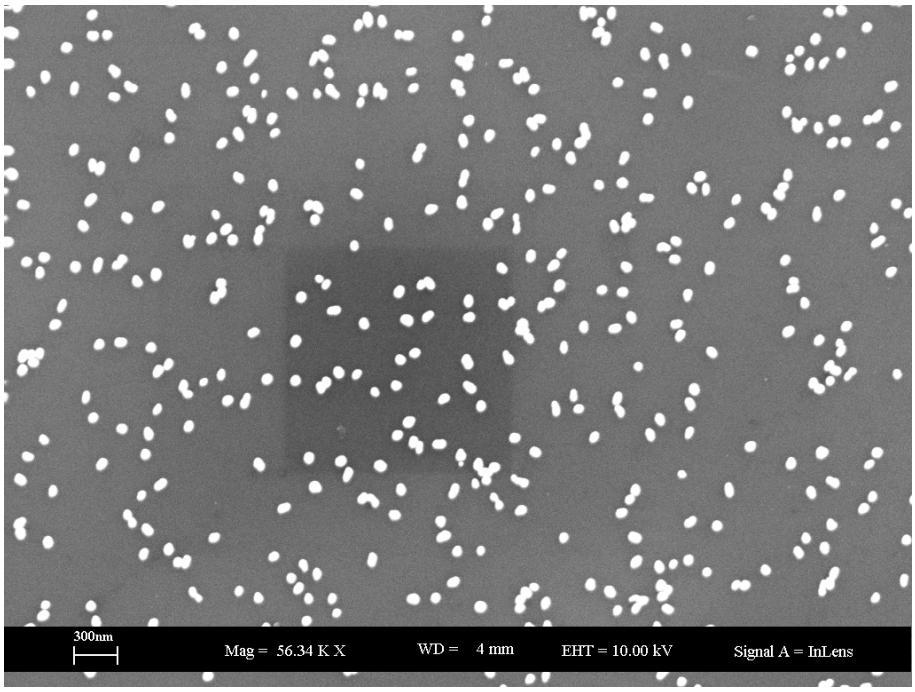

Figure 9: SEM image of the particles used.

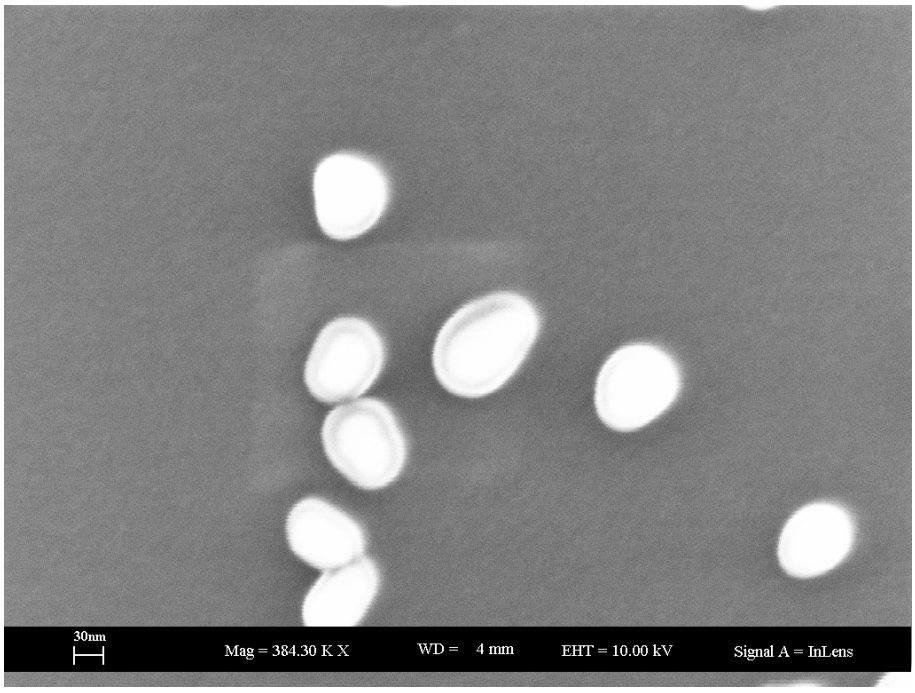

Figure 10: SEM image of the particles used.

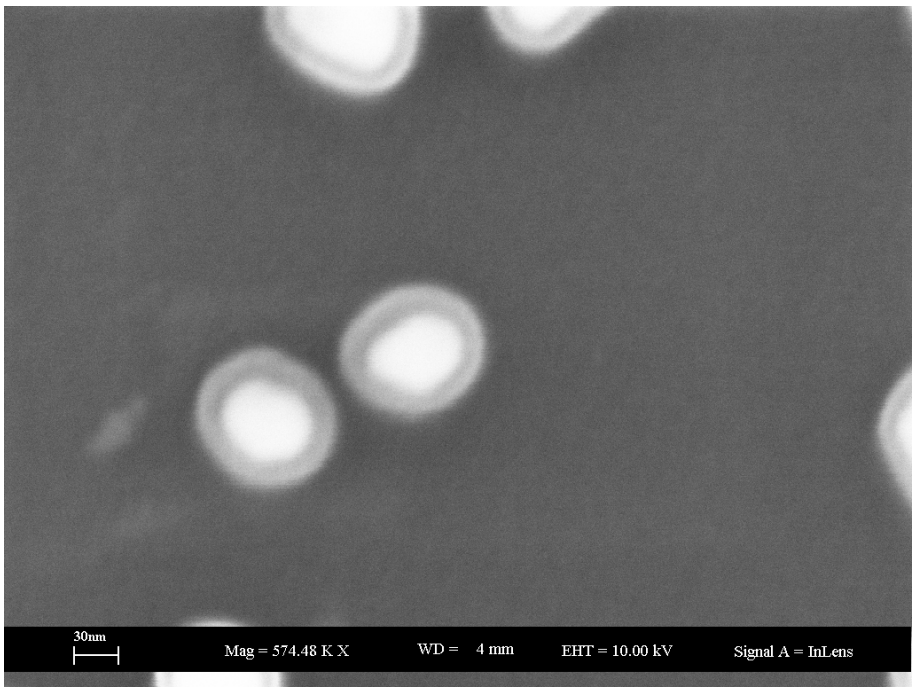

Figure 11: SEM image of the particles used.